Request for Funds for Construction of the BES-III TOF Calibration System

Submitted by the University of Hawaii
on Behalf of the BES Collaboration

October 18, 2005

Abstract

The BEPC e^+e^- storage ring and the BES detector have made important contributions to our understanding of the τ-lepton and charmed quark systems. For instance, measurements of

$$R = \sigma(e^+e^- \to hadrons)/\sigma(e^+e^- \to \mu^+\mu^-),$$

crucial for determining the hadronic contribution to the vacuum polarization in the BEPC energy region, have had a profound impact on the determination of α_{QED} at the mass scale of the Higgs Meson, tests of the Standard Model at LEP, and the Standard Model prediction of the Higgs mass. Currently BEPC and BES are being upgraded to BEPCII/BESIII. The design luminosity of BEPCII is 1×10^{33} cm^{-2} s^{-1}. It will be positioned to make important measurements in the tau-charm energy region.

This proposal is for funds to build a TOF calibration system, which is essential for the successful calibration and monitoring of the BESIII TOF system, essential for π/K separation. The total request for US funding is $320,052 for three years. To meet the proposed summer 2006 installation, we need to begin assembly and testing early in fall 2005.

Contents

1 Introduction **4**
1.1 BES 4
1.2 Hawaii Role in BES 5
1.3 More information 5

2 BESIII - Physics Motivation **6**
2.1 Study of Electroweak Interactions 7
2.1.1 Precision Measurement of CKM Matrix Elements . . . 7
2.1.2 Lepton Universality 8
2.2 Study of Strong Interactions 9
2.2.1 Precision Measurement of Basic QCD Parameters . . . 9
2.2.2 Study of the Light Hadron Spectroscopy 10
2.2.3 Charmonium Physics 11
2.3 Search for New Physics 12
2.3.1 J/ψ Decays 12
2.3.2 D Decays 13

3 Physics reach of BESIII **14**
3.1 Event statistics 14

4 BEPCII **15**

5 BESIII Detector **17**

6 TOF **19**
6.1 Analysis of Time Resolution 20
6.2 Capability of Particle ID 23
6.3 Experience of BESII and BELLE 25
6.4 Choice of Scintillator and PMT 26
6.4.1 Scintillator 26
6.4.2 PMT: R5924 27
6.5 Beam Tests 27
6.6 Simulation 30
6.7 Design 30

7 TOF Laser Timing Calibration System. 35
7.1 Laser 37
7.1.1 Nitrogen dye laser 37
7.1.2 Laser diodes 37
7.1.3 Laser beam measurements 42
7.2 Optical fibers 42
7.3 Tests of calibration system and TOF counters 44

8 The BES TOF Collaboration 44

9 Schedule 45

10 Budget Discussion 45

11 Summary 46

1 Introduction

1.1 BES

The Beijing Spectrometer (BESI) first began operation in 1989. It was a large solid angle multi-particle spectrometer based on a 4.5 kilogauss solenoid magnet operating at the Beijing e^+e^- storage ring (BEPC) at the Institute of High Energy Physics (IHEP) in Beijing. The BEPC energy range spanned the charm- and τ-pair thresholds, making BESI the only experiment then that had the capability of addressing a variety of important physics questions. For example, using production measurements around $\tau^+\tau^-$ threshold, BESI was able to measure the τ mass with an order of magnitude improvement in precision over previous work, thus clearing up a long-standing discrepancy with Standard Model predictions [1]. BESI also accumulated a 3.8M event sample of $\psi(2S)$ decays that enabled the study of decays of charmonium states and a precise measurement of the $J/\psi \to \ell^+\ell^-$ branching fraction [2]. It also accumulated a 22 pb^{-1} sample of $\psi(4.03)$ decays, primarily to study D_s physics.

Several US institutions joined the collaboration in 1991. The US members participated in an upgrade of the BES detector (BESII), coincidental with an upgrade of BEPC. The upgrade was completed in early 1996.

In 1998 and 1999, BESII carried out a detailed R-scan, measuring R at 91 center of mass energies between 2.0 and 4.8 GeV. The R measurements reduced the errors in this energy region from 15 - 20 % to an average uncertainty of 6 % [3, 4]. These measurements were used to determine a new, more precise value of α_{QED} at the Z-pole and a Standard Model Prediction for the Higgs mass, which was shifted upwards from an embarrassingly low 50 GeV/c^2 to 98 GeV/^{2}, more consistent with the lower limit on the Higgs from direct searches at LEP. BESII also obtained samples of 58 million J/ψ events, 14 million $\psi(2S)$ events, and 27 pb^{-1} at the ψ''. These samples have led to a large number of publications.

In 2002, the CLEO collaboration which could no longer compete with the B-factory experiments decided to install wiggler magnets and to lower their energy into the same energy region as BES [5]. Their goal is a luminosity of a few times 10^{32} cm^{-2} s^{-1}, much higher than the BEPC. In addition, the CLEO detector is a well calibrated, high precision detector, much better than the BESII detector.

This forced IHEP to rethink their upgrade plans and to propose a higher luminosity collider with an additional ring (BEPCII) and a brand new detector (BESIII). The goal of BEPCII is 10^{33} cm^{-2} s^{-1}. The proposal was subsequently approved by the Chinese government in 2003.

1.2 Hawaii Role in BES

Hawaii joined the BES collaboration in 1993 and has had a large impact on the BES program. Our group analyzed the $\psi(2S)$ and the 4.03 GeV data samples and took a leading role in the R_{had} measurements. For the BESII detector upgrade, we prepared a laser/fiber-optic calibration system for the new time-of-flight detector and were responsible for the front-end electronics for the new BES vertex detector, which was built around the old Mark III beryllium beampipe by Colorado State University collaborators. We provided new, more compact preamplifier cards for the inner main drift chamber (MDC) layers that were needed to accommodate the reconfiguration of the high voltage for the MDC repair. Our group was responsible for the fabrication of the endplates and the outer cylinder of the replacement MDC for BESII (MDCIII).

At present, Hawaii BES members are Harris, Olsen, Varner, a postdoc Guo, and a graduate student Ong. Currently Harris is the US Co-spokesman. Although small, the group plays an important role. We are responsible along with a few Chinese physicists in the US for internal refereeing (one referee out of three total) most BES papers. In addition, we rewrite most papers for English (and physics) before they are submitted to journals.

Hawaii proposes to use its experience in building TOF calibration systems for BESII and Belle to build a similar system for BESIII. This includes assembling a laser, beam splitter, and reference photo tubes, as well as designing control electronics and developing control and calibration software.

1.3 More information

Much more detailed information is contained in the full BEPC/BESIII proposal, which is available at http://bes.ihep.ac.cn/bes3/design/. Further physics justification is available at
http://www.lns.cornell.edu/public/CLEO/spoke/CLEOc/ProjDesc.html.

2 BESIII - Physics Motivation

The success of the Standard model, especially of electroweak interactions, has been confirmed by many precision measurements performed at LEP and elsewhere. New physics is expected either at higher energies or from precision measurements at lower energies. The former are represented by currently running experiments at the Tevatron and future ones at the LHC, while the latter by "factory" experiments, such as KLOE at the ϕ factory DAfNE and those at the B-factories at KEK and SLAC. The ϕ factory mainly studies the strange quark, and the B-factories are focused on the study of CP violation of the third generation b quark. At the energy region in between, namely the τ-charm energy region, a high luminosity accelerator is still not realized although it was proposed since the 80's of the last century.

Another component of the standard model - quantum chromodynamics (QCD), has been tested extensively at high momentum transfer by many high precision experiments, while at low energies, it is rather difficult to be tested due to its non-perturbative nature. In particular, gluonic matter like glueballs and hybrids, have not been predicted with a clear list of distinctive properties, although they are a straight forward prediction of the non-abelian nature of QCD theory. Lattice QCD (LQCD) can, in principle, give correct predictions for any strong process, but unfortunately, it is limited by computing power and some technical difficulties. LQCD calculations are expected to approach a precision of a few percent in a few years, which will help the comparison between theory and experiments. In the mean time, the reliability of the LQCD calculations should be checked and calibrated by high precision measurements. Charmed mesons, tau leptons, and charmonium states lie in the important energy region where LQCD plays an important role; therefore experimental studies of those physics topics, which can be both measured and calculated with high precision, are extremely important in developing LQCD.

The upgrade of BEPC/BESII to BEPCII/BESIII with a peak luminosity of at least 10^{33} cm^{-2}s^{-1} will certainly provide the possibility of high precision measurements in these two physics areas

2.1 Study of Electroweak Interactions

The BESIII experiment working in the tau-charm energy region will test electroweak interactions with a very high precision in both the quark and lepton sectors.

2.1.1 Precision Measurement of CKM Matrix Elements

Quarks coupling to the weak interaction intermediate bosons are not mass eigenstates. This phenomena results in a transition matrix between weak interaction eigenstates and quark mass eigenstates. This was first proposed by Cabibbo [6], and extended by Kabayashi and Maskawa to three-generations [7]. The matrix is then called the CKM matrix,

$$\begin{pmatrix} d' \\ s' \\ b' \end{pmatrix} = \begin{pmatrix} V_{ud} & V_{us} & V_{ub} \\ V_{cd} & V_{cs} & V_{cb} \\ V_{td} & V_{ts} & V_{tb} \end{pmatrix} \begin{pmatrix} d \\ s \\ b \end{pmatrix}$$

where $\begin{pmatrix} d' \\ s' \\ b' \end{pmatrix}$ are the weak interaction eigenstates, $\begin{pmatrix} d \\ s \\ b \end{pmatrix}$ are the mass eigenstates, and V is a unitary matrix, which can be expressed by three mixing angles and one phase. As basic parameters of the standard model, the precision measurement of the matrix elements is of fundamental importance.

Among those matrix elements relevant to the charm quark, V_{cs} and V_{cd} can be measured from pure leptonic or semileptonic decays of D_s and D mesons, and a precision of 1.6% and 1.8% can be achieved, respectively, at BESIII due to the large statistics and very high purity. V_{cb}, which can be measured from B decays with D or D^* mesons in the final states, will benefit from the high precision measurements of the absolute D decay branching fractions, so as to reduce the error from the tagging modes of B decays. With the combined efforts of both B factories and an unquenched LQCD calculation of the form factor, V_{cb} can be measured to a precision of 3%.

In determining the matrix elements V_{td} and V_{ts} from measuring $B_d\overline{B_d}$ and $B_s\overline{B_s}$ mixing, the decay constants f_{Bd} and f_{Bs} from theoretical calculations are used, since direct measurements of these two quantities are impossible at the moment. The best way to improve the precision of the decay constant calculation is to calibrate the LQCD calculation of the decay constants of

D and D_s, – f_D and f_{D_s} with high precision measurements. From the pure leptonic decays of D and D_s, these decay constants can be measured to a precision of 2% or less; this will help to improve the precision of V_{td} and V_{ts} measurements.

Since there are only four free parameters in the CKM matrix, the high precision measurements of all the matrix elements can be used as a check of the unitarity and normality condition of the matrix. Any significant deviation of measured values from expectation may indicate the incompleteness of the CKM matrix, so as to give a hint of new physics. Otherwise, if matrix elements satisfy all the requirements of the standard model, the mixing angles and the phase can be extracted from the measured values, and a higher precision transition matrix can be obtained.

2.1.2 Lepton Universality

Due to the high selection efficiency and the high purity of the $\tau^+\tau^-$ sample at the Z_0 peak, tau physics at the Z_0 has the advantage of small systematic error for channels with large branching fractions. While at B factories, the large statistics of the $\tau^+\tau^-$ sample makes the study of channels with small branching ratios as well as the search for rare decays and new physics more suitable. $\tau^+\tau^-$ threshold, however, has its own advantages due to the fact that $\tau^+\tau^-$ pairs are produced at very low velocity. They can be used for special physics studies, including the precision measurement of the tau lepton mass for the test of lepton universality and interaction properties between the slowly moving tau pairs produced near threshold.

Lepton universality is a basic, but very strong assumption in the standard Model. The assumption has been tested to very high precision with pure leptonic and semi-leptonic decays of taus and muons. In testing the lepton universality with tau decays, the uncertainty due to the tau mass is now comparable with those due to the tau lifetime and the tau leptonic branching ratios. Following the procedure of the tau mass measurement at BESI with the cross section measurement near the threshold, but with much larger statistics, BESIII can achieve a precision of 0.1 MeV, an improvement of a factor of three compared with the current world average.

It should be noted that the $\tau^+\tau^-$ cross section near the threshold has been calculated to $O(\alpha^4)$ in theory, taking into account initial state radiation, the Coulomb interaction between the taus, and the high precision vacuum

polarization estimation from the hadronic contribution. The precision is supposed to be better than 0.1% [8], which guarantees the final precision of the tau mass measurement where the observed $\tau^+\tau^-$ production cross section as a function of tau mass is fit to the theoretical calculation. At the same time, the measured cross section can be used to test the theoretical calculation of the cross section, especially the non-relativistic QED (NRQED) calculation of the $\tau^+\tau^-$ interaction. This will provide a better understanding of the $\tau^+\tau^-$ interaction near threshold.

2.2 Study of Strong Interactions

Due to the non-perturbative nature of the strong interaction in the tau-charm energy region, almost all theoretical calculations in this energy range have large uncertainties. LQCD will provide high precision predictions in a few years, but due to the limitation of computing capacity and complexity, the results are still very limited. As a consequence, phenomenological models will continue to play an important role in some cases for the interpretation of experimental results. The study of QCD in the tau-charm energy region includes: determination of basic QCD parameters such as the strong coupling constant α_s, the mass of the charm quark m_c, high precision measurements of light hadron spectroscopy, searching for gluonic states such as glueballs and hybrids, and the study of charmonium physics by measuring the production and decay properties of the charmonium states to test and develop QCD calculations.

2.2.1 Precision Measurement of Basic QCD Parameters

In principle, the strong coupling constant can be measured in any strong interaction process provided there are good measurable quantities and reliable theoretical calculations. At BESIII, the most probable processes which may give high precision measurements include: inclusive J/ψ radiative decays, τ decays, and hadronic cross section measurements (R values).

The value of α_s at the c-quark mass can be measured with inclusive J/ψ radiative decays, but the precision depends strongly on that of the theoretical prediction, as well as that of the charm quark mass. The former problem is expected to be taken care of by LQCD, while the latter one can be determined by much more accurate charmonium spectroscopy and high precision

theoretical calculations.

The measurement of α_s with tau decays currently gives the best precision at a mass scale as low as the tau mass, by using high precision measurements of the leptonic branching ratios and spectral functions, with the help of the Operator Product Extension in the theoretical calculation. Although it is hard to improve the tau decay branching ratios at BESIII, the measurement of the spectral function with different systematic effects from previous experiments will contribute to the estimate of the strong coupling constant at the tau mass.

Because QCD only contributes to the correction term of the R value, it is not easy to get a high precision α_s measurement with R data. However since the statistical error at BESIII for the R value measurement at any energy point will be completely negligible and systematic errors excluding common ones are small, the running of the strong coupling constant in the tau-charm energy region can be tested with high precision.

Furthermore, a high precision measurement of R can be used to further improve calculations of the hadronic contribution in vacuum polarization, so as to decrease the systematic uncertainties in the calculation of the abnormal magnetic moment of muon, $a_\mu = (g-2)_\mu$, and the running of the fine structure constant, α, etc.

2.2.2 Study of the Light Hadron Spectroscopy

Hadronic states are the basic components of QCD at low energies; they reflect the strong interaction between quarks within the states. Although the study has a very long history, the understanding of the nature of interactions is rather poor. In addition, QCD predicts the existence of gluonic states like glueballs and hybrids, which have not been experimentally observed or identified unambiguously. This is a hot topic in particle physics.

Radiative decay of the J/ψ is considered as one of the best places for glueball production. Since glueballs are in the same mass range as normal hadronic states, and there is no clear signature predicted, their identification is very difficult, although candidates have been reported. At BESIII, the J/ψ sample will be two orders of magnitude more than that currently collected, and the detector will have better acceptance and resolution. A much more sophisticated partial wave analysis (PWA) for interesting decay channels can be performed. It will be possible to systematically study the production and

decay properties of glueball candidates and search for new ones. At the same time, other QCD predicted non q-qbar states like hybrids and four-quark states can be searched for and studied with J/ψ decays. As an important by-product, systematic studies of normal meson states, high precision measurements of resonance parameters, production and decay properties of light mesons will play an important role in the testing and development of the QCD in the non-perturbative domain, especially in the development of the LQCD to which the high precision data will be a good calibration. The experimental study of the baryonic states with J/ψ data and possibly other charmonium decays will result in a better understanding of the strong interactions between mesons and baryons.

It should be noted that, although glueballs are expected to be substantially produced in J/ψ radiative decays, the study of other hadronic states can be done in a very different environment, such as in J/ψ hadronic decays, non-leptonic decays of D or D_s mesons, the decays of $\psi(2S)$ and charmonium production from $\psi(2S)$ decays, as well as the semi-leptonic decays of the tau lepton.

2.2.3 Charmonium Physics

J/ψ, $\psi(2S)$, $\psi(3770)$, and the charmonium states formed from their decays can be used to test QCD by measuring their production and decay properties with the large data samples. The potential model and the non-relativistic QCD (NRQCD) color-octet mechanism play important roles in production and decay of quarkonium states, and detailed information of the theory, including some crucial input parameters like the color-octet matrix elements need to be determined from experiments. A systematic study of the charmonium states below open charm threshold will hence provide theoretical input parameters and further test other predictions from the theory.

The P wave spin singlet $^1P_1$ was discovered recently by E835 [9] and CLEOc [10], but much larger data samples are required to better understand the detailed properties of this state. The precise measurement of the $^1P_1$ mass will provide an important test of the Dirac structure of the quarkonium potential. High precision measurements of the resonance parameters of all charmonium states, together with their production rates and decay modes, will supply substantial experimental information for testing theoretical models.

It should be noted that the large data samples collected at the B factories are being used for the charmonium physics studies, including the discoveries of charmonium states, but the systematic study of these states will be better at BESIII since the data sample will be much larger and the background level lower.

The study of the charmonium decay dynamics is another important topic. It has been revealed that the charmonium spin-triplet state J/ψ and its radially excited state $\psi(2s)$ have very different decay patterns in some hadronic channels, compared with the naive QCD prediction. The vector-pseudoscalar (VP) decays of $\psi(2s)$ were found to be significantly suppressed - the so called "rho pi puzzle". Further experimental studies show that not only the VP mode, but also the vector-tensor (VT) decay mode is suppressed, although the suppression is weaker. Current experimental studies are still limited by statistics. At BESIII, the large data samples at the J/ψ, $\psi(2S)$, and $\psi(3770)$ resonances and the nearby continuum will allow the measurements of all the interesting hadronic decay modes to a level similar to that of electromagnetic interactions, and different decay rates of these three charmonium states with different quantum numbers can be compared after non-resonance contributions are subtracted. It may then be possible to understand QCD in charmonium decays and to understand finally the "rho pi puzzle".

2.3 Search for New Physics

Rare decays and processes not allowed by the standard Model can be searched for with the high statistics data sample to detect or give constraints on new physics. At the tau-charm energy region, there are many possibilities to search for new physics. Here we only list the single D_s or D production, lepton and baryon number violation processes in J/ψ decays, mixing, and flavor changing neutral currents (FCNC) with D data.

2.3.1 J/ψ Decays

In the standard model, weak decays of the J/ψ to single D_s or D mesons have a branching ratio on the order of 10^{-8}. At BESIII, with 10^{10} J/ψ events in one year's running, the decays can be observed, and the theoretical prediction can be tested. Most importantly, if the observed production rate

deviates significantly from expectations, it indicates the existence of other dynamics, or new physics.

In the standard model, lepton number and baryon number are conserved exactly. Very stringent limits have been set from $Z_0 \to \tau$ and μ decays. With the large data sample at BESIII, the upper limits of $J/\psi \to e\mu, e\tau, \tau\mu, ep, \mu p, \tau p$, etc. can be set to the level of 10^{-9}, to give stringent limits for theories beyond the standard model, or restrict the parameter space of non-standard models.

It was pointed out long ago that the spin correlation between two separated spin half particles can be used to measure Bell's inequality to test quantum theory [11]. A few hundred $\eta_c \to \Lambda\bar{\Lambda}$ events are expected to give good test precision, while a much larger $\eta_c \to \Lambda\bar{\Lambda}$ sample can be obtained at BESIII. A careful study will give an unambiguous answer to the question, and supply the first test of the Bell's inequality in particle physics.

2.3.2 *D* Decays

The Standard Model predicts a very small mixing probability and small direct CP violation in D_s and D decays, while new physics may enhance the effect dramatically. A careful study of mixing from $\psi(3770)$ decays can reach a mixing probability of 10^{-4}, which, although still far away from the standard model prediction of 10^{-9}, gives a constraint on new physics contributions.

A new physics search can also be performed through the measurement of FCNC decay modes. The standard model predicts the decay rates of $D \to \pi e^+ e^-, \pi\mu^+\mu^-, \rho e^+ e^-, \rho\mu^+\mu^-$ being on the order of 10^{-6} [12], which can be reached with BESIII statistics. The test of these predictions with experimental measurements will reveal possible effects due to new physics.

In summary, the construction of a high luminosity accelerator and high performance detector in the tau-charm energy region opens a new window for high precision measurements of electroweak interactions through the study of the charm mesons and tau leptons, the high precision study of the perturbative and non-perturbative QCD with J/ψ and other charmonium decays, and new physics searches. All these studies will supply more high quality tests of the standard model and give constraints to or hints on new physics.

Table 1: Number of events expected for one year of running.

Physics channel	Center-of-mass Energy (GeV)	Peak Luminosity (10^{33} cm^{-2} s^{-1})	Physics cross section (nb)	Number of Events per year
J/ψ	3.097	0.6	~ 3400	10×10^9
τ	3.67	1.0	~ 2.4	12×10^6
$\psi(2S)$	3.686	1.0	~ 640	3.0×10^9
D	3.770	1.0	~ 5	25×10^6
D_s	4.030	0.6	~ 0.32	1.0×10^6
D_s	4.140	0.6	~ 0.67	2.0×10^6

3 Physics reach of BESIII

3.1 Event statistics

The design peak luminosity of BEPCII is 10^{33} cm^{-2} s^{-1} at 1.89 GeV, which is the highest ever planned in the tau-charm region. An unprecedented large number of physics events is expected, giving opportunities to obtain important physics results.

The number of expected events, N, is given by $N = L\sigma T$, where L is the luminosity, σ the cross section of the physics process, and T the integral of the data taking time. In the following calculations, we will use the average luminosity, $L = 0.5L_{peak}$, to take into account the effect of the beam lifetime and injection time. T for data taking is taken as 10^7 seconds per year. In calculating the total cross section, the spread of the center-of-mass energy of BEPCII, σ_E , is taken into account and the maximum solid angle coverage of the detector, $\cos_{max} = 0.93$, is used.

The physics event rates at BEPCII are enormous, about 4300Hz at the J/ψ , 1300Hz at the $\psi(2S)$, and 400-1000Hz for dominant QED processes at other energy points. The number of events accumulated for each kind of physics in one year of running is shown in Table 1.

4 BEPCII

The main physics goals of BEPCII are precision measurements of Charm decays and searches for new particles and new phenomena, mainly in the energy region of the J/ψ to the ψ''. This requires a major upgrade of the BEPC to increase its luminosity by two orders of magnitude. The main parameters of BEPCII are listed in the Table 2 below with a comparison to those of the current BEPC.

BEPCII will be a double-ring collider with super-conducting micro-β magnets, a 500 MHz RF system with super-conducting cavities, a low impedance antechamber beam pipe, and a horizontal large angle crossing of 11 mrad at the southern interaction region. There will be 93 bunches per ring with a total current of 910 mA per ring. The peak luminosity of BEPCII will be 10^{33} cm^{-2} s^{-1} at the beam energy of 1.89 GeV. The peak luminosity at the J/ψ and at 4.1 GeV c.m. energy will be about 0.6×10^{33} cm^{-2} s^{-1}. The upgraded LINAC will provide full energy injection up to 1.89 GeV for top-off injection. The positron injection rate will reach 50 mA/min.

Progress is on schedule. The linac upgrade was completed in October 2004, and the e^- beam was available for synchrotron running in Dec. 2004. The e^+ beam was brought to the end of the linac in March 2005. The current is at design, and the emittance is better than design.

The manufacturing of storage ring components is underway. The Linde compressor and superconducting cavities have arrived, and much of the cryogenic pipe work is complete.

Table 2: Main parameters of BEPCII in comparison with the BEPC.

Parameters	Units	BEPCII	BEPC
Operation energy (E)	GeV	1.0 - 2.1	1.0 - 2.5
Injection energy (E_{inj})	GeV	Up to 1.89	1.3
Circumference (C)	m	237.5	240.4
Revolution frequency (f_r)	MHz	1.262	1.247
Lattice type		FODO + micro-β	FODO + low-β
β^*-function at IP (β^*_x/β^*_y)	cm	100/1.5	120/5
Natural energy spread (σ_e)		$2.73E \times 10^{-4}$	$2.64E \times 10^{-4}$
Damping time ($\tau_x/\tau_y/\tau_e$)		25/25/12.5@1.89 GeV	28/28/14@1.89 GeV
RF frequency (f_{rf})	MHz	499.8	199.533
Harmonic number (h)		396	160
RF voltage per ring (V_{rf})	MV	1.5	0.6 - 1.6
Bunch number (N_b)		93	2 x 1
Bunch spacing	m	2.4	240.4
Bunch current (I_b)	mA	9.8 @1.89 GeV	35 @1.89 GeV
Beam current - Colliding	mA	910 @1.89 GeV	2 x 35 @1.89 GeV
Beam current - SR	mA	250 @ 2.5GeV	140 @ 2.2 GeV
Bunch length (σ_l)	cm	~ 1.5	~ 5
Impedance $\lvert Z/n\rvert_0$	Ω	~ 0.2	~ 4
Crossing angle	mrad	± 11	0
Vert. Beam-beam param. (ξ_y)		0.04	0.04
Beam lifetime	hrs.	~ 2.7	6 - 8
Luminosity@1.89 GeV	10^{31} cm^{-2} s^{-1}	100	1

5 BESIII Detector

BEPCII is a high luminosity, multi-bunch collider, which requires a comparable high quality detector with modern detector technology. A factor of 100 increase in statistics requires a corresponding reduction of systematic errors. The choice of the detector components is based on physics requirements, existing experience in the collaboration, budgetary and schedule constraints, etc. Figure 1 shows the schematic of the BESIII detector, which consists of the following components:

- A He gas based drift chamber (MDC) with a single wire resolution better than 120 μm;
- A CsI calorimeter (EMC) with an energy resolution of 2.5%@1 GeV;
- A Time-of-Flight system with a time resolution better than 90 ps for muons;
- A super-conducting solenoid magnet with a field of 1.0 Tesla;
- A RPC based muon chamber system.

Details of each sub-detector will be can found at http://bes.ihep.ac.cn/bes3/design/. Table 3 shows the comparison of the BESII and BESIII detectors.

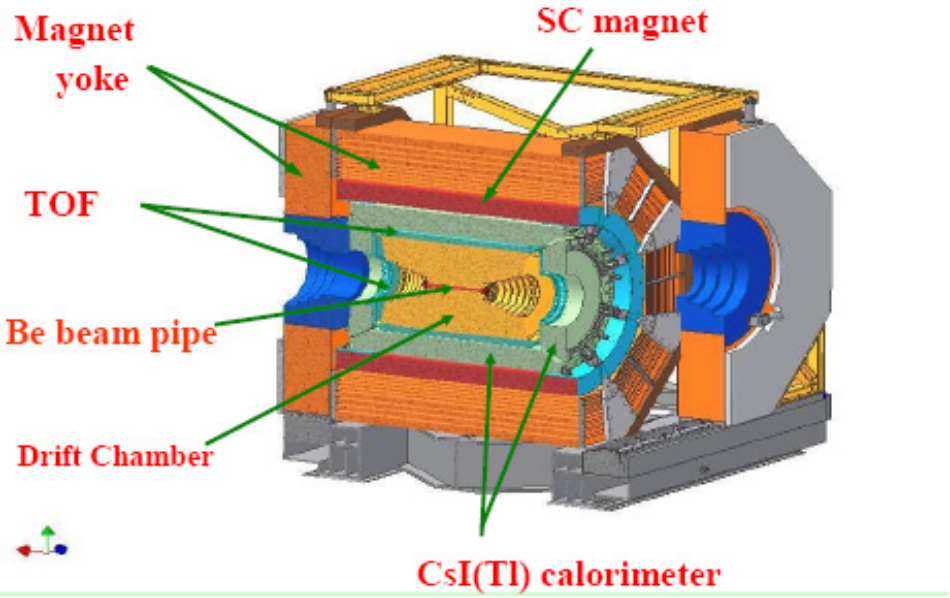

Figure 1: Schematic drawing of the BESIII detector.

Table 3: Comparison of Detector Parameters.

Sub-system	BESIII	BESII
MDC	$\sigma_{xy} = 120\ \mu m$ $\Delta P/P = 0.6\%$ @ 1GeV $\sigma_{dE/dx} =$ (6-7) %	250 μm 2.4%@1GeV 8.5%
EM Calorimeter	$\Delta E/\sqrt{E} = 2.5\%$ @ 1 GeV $\sigma_z = 0.5$ cm @ 1 GeV	20%@1GeV 3 cm @ 1 GeV
TOF detector	$\sigma_T = 90$ ps barrel 110 ps endcap	180 ps barrel 350 ps endcap
μ counters	10 layers	3 layers
Magnet	1.0 tesla	0.4 tesla

The total budget for the BEPCII and BESIII is 640 million Chinese Yuan (about 77M US$), which is provided by the Chinese government. Beam tuning with BEPCII is scheduled to begin in June 2006, and BESIII is scheduled to be installed in Dec. 2006. Data taking is scheduled to take place by summer 2007. At present, almost all items are on schedule, and progress is rapid. Figure 2 shows the completed drift chamber structure in June ready for shipment to IHEP for wiring, and Fig. 3 shows the winding of the superconductor inside the support cylinder of the solenoidal superconducting magnet. The winding was completed in early June 2005.

Figure 2: Completed drift chamber structure ready for shipment to IHEP for wiring - June 2005.

6 TOF

Here more detail is given concerning the TOF system, since this proposal is for a calibration system for the TOF.

The Time of Flight (TOF) detector is used to measure the flight time of charged particles. Particles are identified by comparing the measured time obtained for a track against the predicted times for different particle hypotheses using the momentum measured by the MDC. The particle identification

Figure 3: Winding the superconductor inside the support cylinder of the solenoidal superconducting magnet.

by the TOF system is of extreme importance to the BES experiment. The TOF detector is located between the MDC and EMC (see Fig. 4). The solid angle coverage of the barrel TOF is given by $|\cos\theta| < 0.83$, and that of the endcap TOF is for $|\cos\theta|$ from 0.85 to 0.95. The TOF also provides a fast trigger signal.

6.1 Analysis of Time Resolution

The purpose of the TOF is to identify particles, and its capability is determined by its time resolution, which has the following contributions:

$$\sigma = \sqrt{\sigma^2_{TOF} + \sigma^2_{bunch-time} + \sigma^2_{bunch-length} + \sigma^2_{Z-position} + \sigma^2_{electronics} + \sigma^2_{expect} + \sigma^2_{time-walk}}$$

- σ_{TOF}, intrinsic TOF time resolution.

  The intrinsic time resolution of the TOF is determined by the scintillator and PMT characteristics by the following formula [13],

$$\sigma_{TOF} = \sqrt{\frac{1}{(2.35)^2}\{\tau^2_{scin} + [\frac{n(n-1)L}{2c}]^2 + \tau^2_{PMT}\}}/\sqrt{N_{pe}}$$

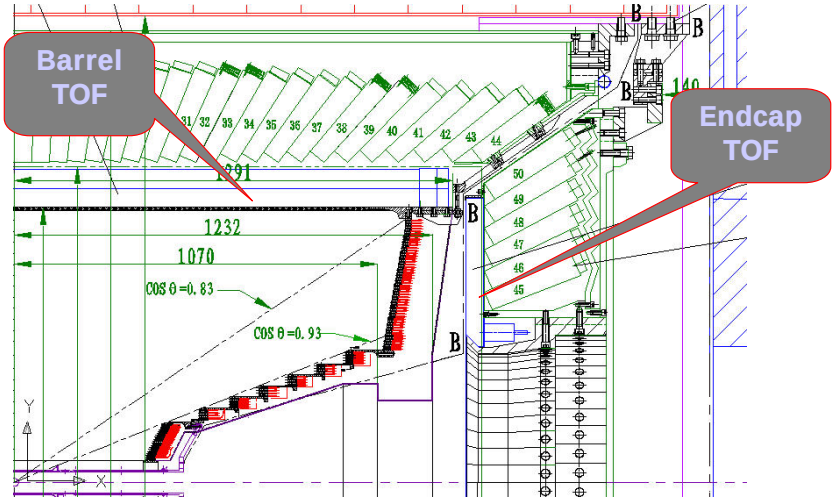

Figure 4: Time Of Flight System.

Here, τ_{scin} is the decay time of the scintillator, n the refractive index, L the distance from the hit position to the PMT, τ_{PMT} the time jitter of the PMT for a single pe (photo-electron), and N_{PE} the number of the pe's detected. N_{PE} depends on the scintillation light output, its attenuation length, and the quantum efficiency of the PMT as given by the following formula:

$$N_{PE} \propto \int N_0(\lambda) L_t e^{-L_t/L_a} \epsilon(\lambda) d\lambda$$

where λ is the light wavelength, $N_0(\lambda)$ is the scintillator light output per unit thickness, L_t is the path length of the particle in the scintillator, L_a is the attenuation length of the scintillator, and $\epsilon(\lambda)$ is the quantum efficiency function of the PMT. From this formula and our experience and that of Belle, the intrinsic time resolution is expected to be better than or equal to 80 ps for a single TOF layer (see Sections 6.3 and 6.5).

- $\sigma_{bunch-time}$, from the beam bunch timing uncertainty. The time resolution is degraded by the uncertainty of the bunch timing with respect to a global timing marker (e.g. RF clock). There will be 93 beam bunches at the same time and the phase resolution of beam bunches from the

RF is about 1 deg, for a RF period of 2 ns. Thus the intrinsic bunch timing resolution is about 5 ps. A further degradation occurs due to the jitter in registering the TOF timing measurements with respect to the global timing marker and in the readout electronics. The bunch timing uncertainty is expected to be about 20 ps including differences due to cables.

- $\sigma_{bunch-length}$, from the bunch length uncertainty. Electrons and positions collide in beam bunches, and their collision time depends on the bunch time and bunch length. According to the design of BEPCII, the bunch length is 1.5 cm, i.e., 50 ps. Considering the collision of two bunches, the uncertainty will be reduced by a factor of $\sqrt{2}$, which is 35 ps.

- $\sigma_{z-position}$, from the Z-position uncertainty. The transit time in the scintillator depends on the uncertainty in the Z-position of the particle impact. According to the MDC track reconstruction, the Z-position uncertainty is about 0.5 cm, taking into account the refractive index of scintillator of about 1.5, which corresponds to a 25 ps timing error.

- $\sigma_{electronics}$, from the electronics of the time measurement. The electronics of the time measurement of TOF will use the CERN HPTDC chip whose resolution is better than 25 ps according to its design.

- σ_{expect}, from the resolution of the expected time of flight.

  The capability of particle identification is determined by the difference of the measured time and expected time. So the resolution of the expected time of flight, which is determined by the MDC track length and momentum resolution will directly affect Particle ID. The momentum resolution is better than 0.6% for 1 GeV/c tracks, and the track length resolution should be several millimeters from our simulation. Thus σ_{expect} will be about 30 ps.

- $\sigma_{time-walk}$, from the time walk effect. A double threshold scheme will be used to suppress background and reduce the time-walk, similar to the scheme used by Belle [14, 15]. The high threshold (about 250 mV) is used to gate an ADC used to determine the pulse height, while the low threshold (about 50 mV) is used to measure the time. The time value

Table 4: Analysis of TOF time resolution for muons

Item	Barrel time resol.	Endcap time resol.
Intrinsic time resol. of one TOF layer	80 - 90 ps	80 ps
Uncertainty from bunch length	15 mm, 35 ps	15 mm, 35 ps
Uncertainty from bunch time	$\sim$ 20 ps	$\sim$ 20 ps
Uncertainty from Z position	5 mm, 25 ps	10 mm, 50 ps
Uncertainty from electronics	25 ps	25 ps
Resolution of expected time of flight	30 ps	30 ps
Time walk	10 ps	10 ps
Total time resol, one layer of TOF	100 - 110 ps	110 - 120 ps
Total time resol, double layer of TOF	90 ps	

is then corrected using the ADC value in a time-walk correction. The ADC resolution (least count) yields a time-walk correction uncertainty of about 10 ps.

In total, a double-layer scintillator barrel TOF is expected to have 90 ps time resolution, as detailed in Table 4.

The Barrel TOF will be composed of two scintillator layers with PMTs. MRPCs are being investigated as an alternative for the second layer, but will not be used initially. A big MRPC (2400mm long and 100mm wide) is currently being tested.

The endcap TOF will use fan-shaped scintillators instrumented with PMTs at the inner radius. Although the width of the scintillator increases and the readout is only on one end, the total scintillator length is only about 40 cm. Hence, the intrinsic time resolution is still below 80 ps. Since the particle hit position will be not determined as precisely as for the barrel, a 50 ps timing uncertainty is expected for an estimated 10 mm error. In summary, the endcap TOF is expected to have a time resolution of about 110 ps.

6.2 Capability of Particle ID

The flight time difference, ΔT, between a K and π with the same momentum can be estimated from the BESIII dimensions. Comparing ΔT with

the TOF time resolution, an estimate can be made for the K/π separation capability. If we assume the flight time measurement is described with a Gaussian distribution, a 2σ separation corresponds to $\Delta T > 3.38\sigma$, and a 3σ separation corresponds to $\Delta T > 5.60\sigma$. The time resolution is a function of the hit position in the scintillator, which follows the following formula based on our experience:

$$\sigma(x) = \sigma(0)(1 - 0.3x^2),$$

where $x = \cos\theta$, θ is the polar angle, and $\sigma(0)$ is the time resolution at the middle of the scintillator.

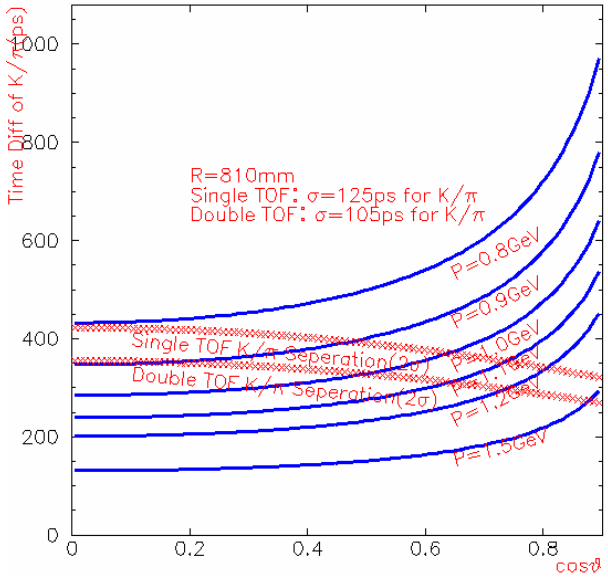

Figure 5: Kaon and pion separation.

The time resolution of one scintillator layer for muons in the barrel TOF is about 100 - 110 ps. For kaons and pions, it will increase by 20% because of strong interactions, as experienced at BESI, BESII, and BELLE. For a double-scintillator-layer TOF, the intrinsic time resolution is reduced by a factor of $\sqrt{2}$, hence $\sigma(0) = 105$ ps. Fig. 5 gives the K/π separation capability, calculated from the above formulae, for a one layer or double layer TOF. The 2σ K/π separation momentum is 0.8 GeV/c for a single layer TOF and 0.9 GeV/c for a double layer TOF.

6.3 Experience of BESII and BELLE

The BESII [16] TOF system was constructed from 1994 to 1996. Its barrel consisted of 48 BC408 scintillation counters, 284 cm long, 15.6 cm wide, and 5 cm thick. Each scintillator was connected to a 16 cm long fish-tail shaped light guide coupled to a round light guide and coupled to a 2" PMT. The ratio of the effective area of the PMT to scintillator was only 16%. The PMTs used were Hamamatsu R2490-05, with fine-mesh dynodes and a gain of up to 3×10^6 at no magnetic field (0T) and 1×10^6 at a magnetic field of 0.5 T.

The total time resolution of the BESII TOF was 180 ps, where the intrinsic time resolution was 135 ps while another 125 ps error came mainly from the bunch length of the beam. Because the radius of MDC was large, 115cm, the momentum upper limit for K/π separation was 0.8 GeV/c, as shown in Fig. 6.

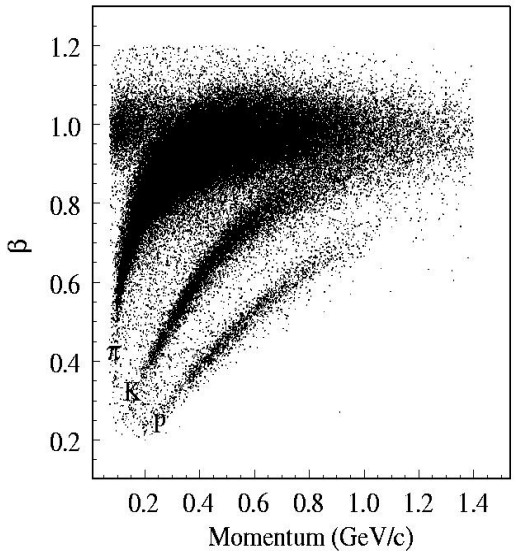

Figure 6: Velocity versus momentum of particles in BESII.

The Belle TOF [14] detector consists of one layer of thin trigger scintillation counters (TSC) and one layer of TOF scintillation counters. Its TOF scintillators are 255cm long, 6cm wide, and 4cm thick and are directly con-

Table 5: Properties of BC-404 and BC-408

	BC-404	BC-408
Light Output, % Anthracene	68	64
Rise Time, ns	0.7	0.9
Decay Time, ns	1.8	2.1
Pulse Width, FWHM, ns	2.2	$\sim$2.5
Light Attenuation Length, cm	140	210
Wavelength of Max. Emission, nm	408	425
No. Of C Atoms per cm^3, ($\times 10^{22}$)	4.74	4.74
No. Of H Atoms per cm^3, ($\times 10^{22}$)	5.21	5.23
Ratio H:C, Atoms	1.100	1.104
No. Of Electrons per cm^3, ($\times 10^{23}$)	3.37	3.37

nected to PMTs. The ratio of effective area of PMT to scintillator is 50%. The PMT, R6680, was specially designed by Hamamatsu with 24 fine-mesh dynode stages. Its gain is up to 3×10^6 in a 1.5 T field, and its transit time spread is 320 ps (r.m.s.). Total time resolution of Belle TOF reaches 100 ps with the intrinsic part being 70 to 80 ps. The major reason for such a large difference is that the BESII TOF has light guides between the scintillator and PMT, and has hence a small ratio of PMT area to scintillator area and therefore less photoelectrons.

6.4 Choice of Scintillator and PMT

6.4.1 Scintillator

Both BC404 and BC408 scintillators, produced by Bicron, are considered. Table 5 lists their parameters. BC404 has more light output, faster rise and decay times, but a shorter attenuation length. According to our simulation, for a longer scintillator bar, BC408 is better. For the barrel, we will use BC408 by Bicron or EJ200 by Eljen Technology, which has very similar characteristics, as the scintillator. The scintillator for the endcap will be BC404 or EJ204, which again is similar. They have faster rise times.

6.4.2 PMT: R5924

The choice of the PMT depends on parameters such as performance, effective area, gain in a magnetic field, cathode quantum efficiency, and spectral response. Considering the limited space, a shorter PMT is preferred. The Hamamatsu R5924 fulfills most requirements:

- Its diameter is 52 mm, and its cathode diameter is 39 mm (See Fig. 7). For a scintillator cross section of about 50 mm x 60 mm, the effective area ratio is 40%.
- It has 19 fine-mesh dynode stages, and its gain is 1.0 $\times 10^7$ in a 0 Tesla magnetic field, 4.1 $\times 10^6$ at 0.5 Tesla, and 2.5 $\times 10^5$ at 1 Tesla.
- It has high quantum efficiency for light with a wavelength from 300 nm to 500 nm.
- It has good timing performance: the anode pulse rise time is 2.5 ns, transit time 9.5 ns, and transit time spread (FWHM) 0.44 ns.
- Its length is 50 mm.

One shortcoming of the R5924 is that its gain at 1 Tesla is a bit low. To compensate, preamplifiers will be used to amplify the pulses from the PMTs.

6.5 Beam Tests

Electron and pion beams were used to test TOF modules; the setup is shown in Fig. 8. The counters T01 and T02 are used to give a precise reference time, and the Pb wall is used to absorb background radiation. Scintillator bars are connected directly to the PMTs in the dark box. The Cherenkov detector is used to separate electrons and pions. The scintillators S1 and S2 are used for the trigger, and the wire chamber MWPC is used to determine the track position.

Some results are displayed in Fig. 9, which shows a comparison of the time resolution of BC408 with different wrapping materials, where a time resolution less than 90 ps is obtained with aluminum foil wrapping. Figure 10 shows test results for endcap modules using different scintillator materials. Time resolution better than 80 ps is obtained with BC404.

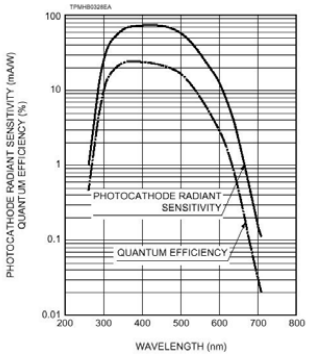

a. Typical Spectral Response

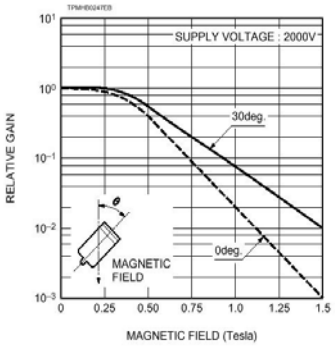

b. Typical Gain in Magnetic Fields

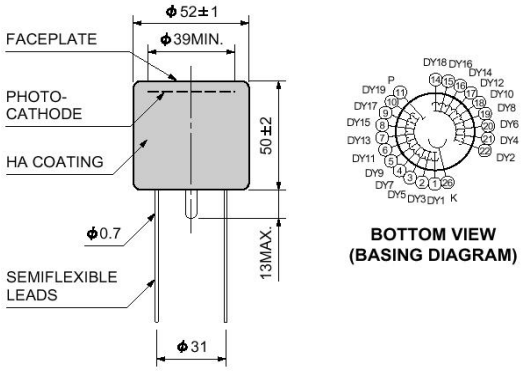

c. Dimensional Outline and Basing Diagram (Unit: mm)

Figure 7: Characteristics of PMT R5924.

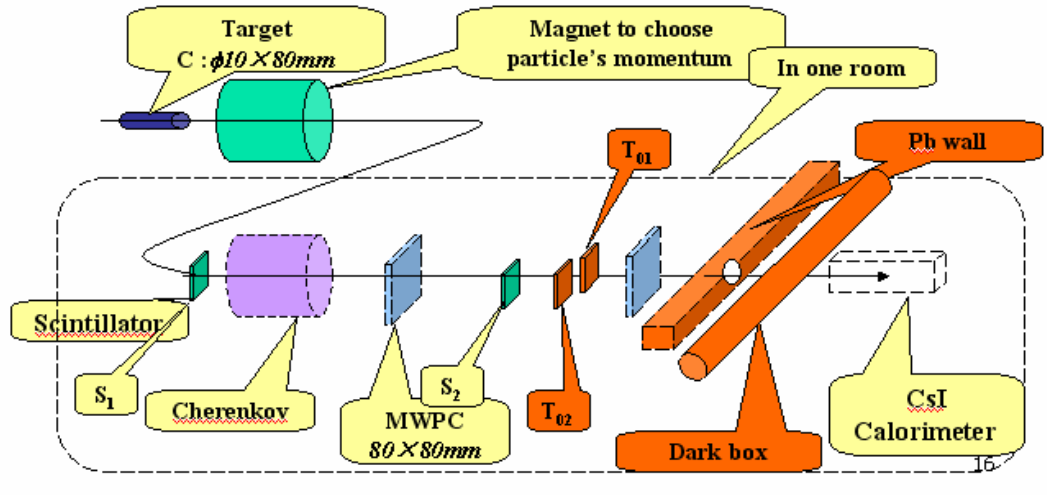

Figure 8: Beam test setup.

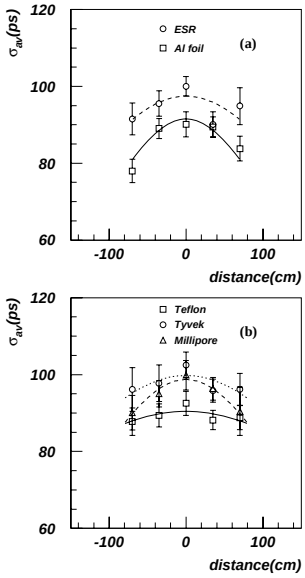

Figure 9: Beam test results: time resolution versus position for various wrapping materials with BC408.

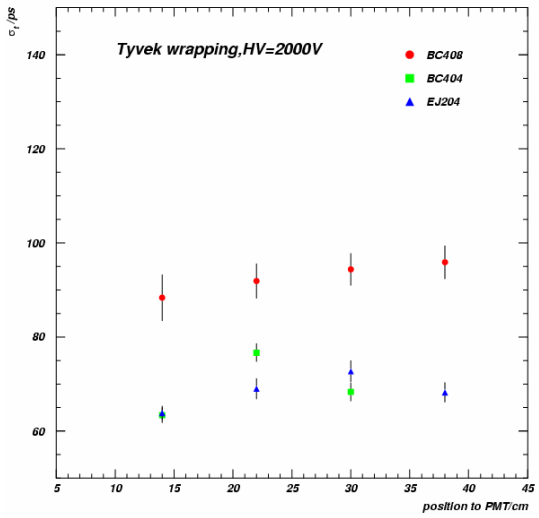

Figure 10: Beam test results: time resolution versus position of endcap modules for different scintillators.

6.6 Simulation

The performance of a TOF module is simulated with GEANT4. Most physics processes are simulated, including the tracking of charged particles, energy deposition, scintillation light production and transport, PMT signal shape, etc. This simulation program has been used to compare BC404 and BC408 and different scintillator thicknesses, threshold value settings, etc. Fig. 11 shows the time resolution determined from the simulation as a function of position for BC404 and BC408, with and without silicon oil between the scintillator and PMT. Simulation indicates the resolution of the weighted mean times is better than 90 ps for BC408. We find good agreement between the TOF resolutions determined from our calculated estimates, the beam tests, and simulations.

6.7 Design

The barrel TOF will be placed between the MDC and EMC. To save space and simplify the setup, the TOF system will be mounted directly on the outside of the MDC. The outer radius of the MDC is 810 mm and the inner

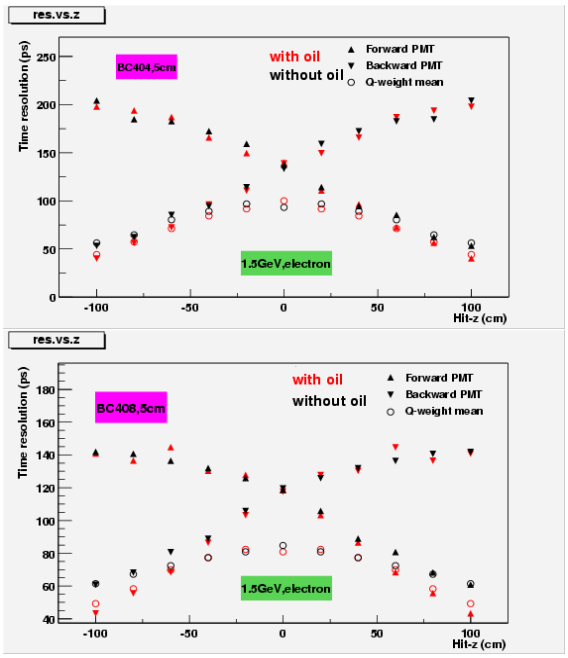

Figure 11: Time resolution from simulation for BC404 or BC408, with or without silicon oil.

radius of the EMC is 930 mm. Thus the TOF has 120 mm of radial space in total, into which two layers of 50 mm thick scintillator and mounting hardware must fit. The TOF will be 2500 mm and 2600 mm long including PMTs, respectively, for the inner and outer layers. Its solid angle coverage is 82% of 4π after subtracting 2 x 80 mm of space for the PMTs. Considering the PMT packing constraints, each layer will have 88 scintillator pieces and weigh approximately 700 kg.

The TOF design will satisfy the following conditions:

- The end of the scintillator should match the PMT so as to maximize the effective area ratio.
- Scintillator should be wrapped to protect it from light leaks.
- The scintillators and PMTs are connected with silicon oil in between.
- The PMT should be independently supported.
- The base of the PMT should be shorter than 30 mm due to the space limitation.
- The maximum radius of the TOF should be less than 925 mm with a clearance of 5 mm, since the MDC and TOF should be installed inside the EMC after they are assembled together.
- The housing of PMT should have good heat exchange to remove the heat from the voltage divider.

Fig. 12 shows the barrel TOF module assembly. The PMTs will be placed in an aluminum alloy housing, and the housing will be screwed to the scintillator ends. A preamp is directly connected to the PMT in the PMT housing.

The barrel TOF installation sequence is as follows:

- Wrap each piece of scintillator with Al foil and black adhesive tape.
- Assemble inner layer of scintillator: first attach a layer of rubber to the MDC outer skin; then attach scintillator to rubber with adhesive tape.
- Assemble outer layer of scintillator: first attach a layer of rubber to the inner layer of TOF; then attach the second layer of scintillator to rubber.

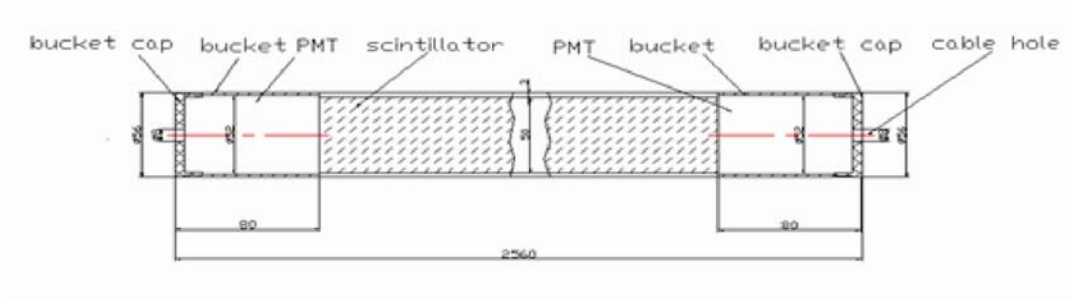

Figure 12: Barrel TOF module assembly.

- Screw PMT support housings to the scintillator and insert PMTs and screw on the housing covers.

The endcap TOF will be placed at both ends of BESIII between the MDC and the endcap EMC. It consists of 48 pieces of fan-shaped scintillator with a thickness of 50 mm and an inner radius of 410 mm and an outer radius 890 mm. To minimize the impact to the acceptance, the PMTs will be connected at the inner end of each scintillator, as shown in Fig. 13.

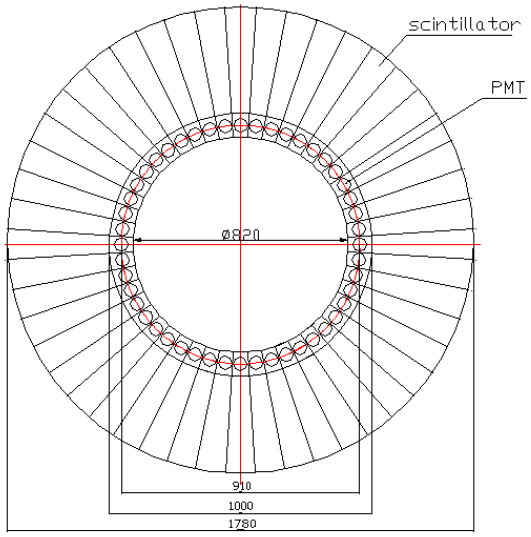

Figure 13: Endcap TOF.

The installation of the endcap TOF will be simple. Each piece of the

scintillator, after it is wrapped with Al foil and black adhesive tape, will be mounted on the endcap EMC. At the center, there will be a metal ring to support the scintillator. The PMTs will be placed in housings, and the base of the housing will be connected to the scintillator by screws, as shown in Fig. 14. Because the endcap must open, the preamps for the endcap PMTs will be put outside of the housings, about 0.6 m away at the back of the endcap EMC. See Fig. 15.

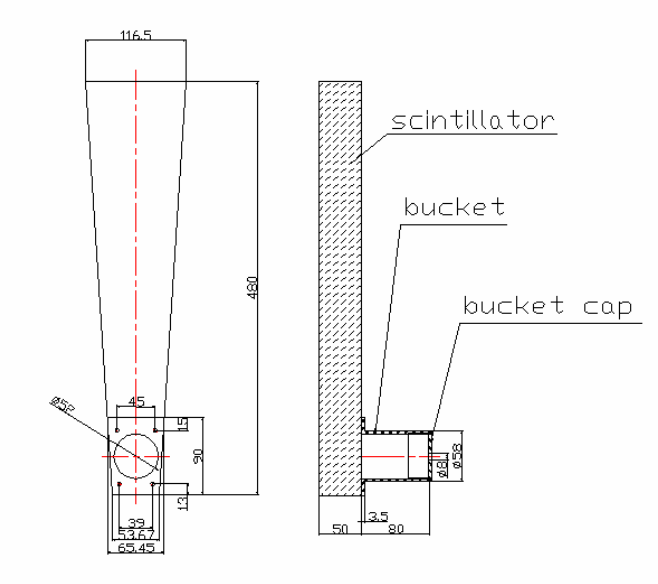

Figure 14: Endcap TOF counter.

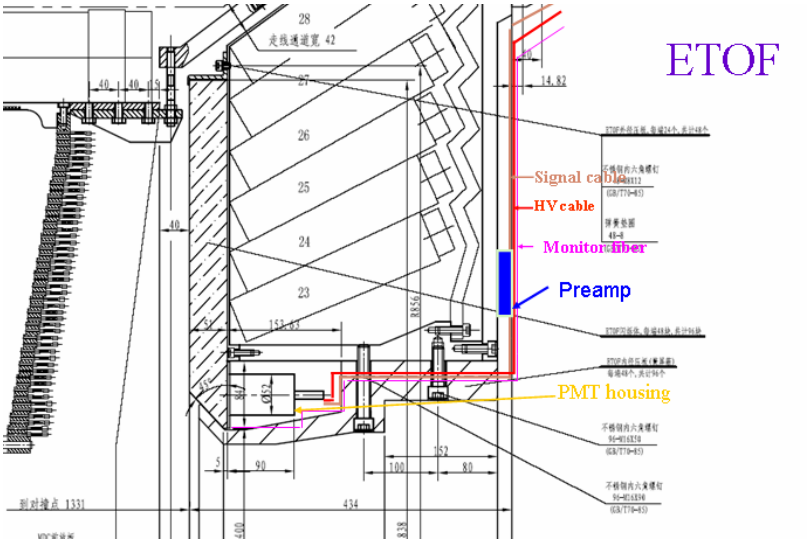

Figure 15: Endcap TOF counter installation.

7 TOF Laser Timing Calibration System.

The Hawaii group will construct a pulsed-laser system that will provide light signals with well defined relative times to each of the TOF scintillators, providing a simple and robust means for adjusting and monitoring the channel-to-channel calibration constants.

Such systems were used in BESII and Belle. Figure 16 shows the BESII calibration system, and Fig. 17 shows the schematic diagram of this system. Laser pulses are injected into one of two bundles of several meters-long optical fiber cables following optical conditioning with appropriate filters and diffusers. One of the bundles is connected to one end of the TOF scintillators, and the other bundle to the other end. A swing beam-steering mirror selects which end is to be illuminated by laser pulses. The beam splitter reflects a small fraction of the laser beam into the reference (T_0) PMT and provides a TDC start signal. The TDC stop signal is supplied by the PMT on one of the TOF ends. The signal is also output to an ADC to record the amplitude. After correcting for the amplitude, the time resolution can be obtained.

Figure 16: BESII TOF calibration system.

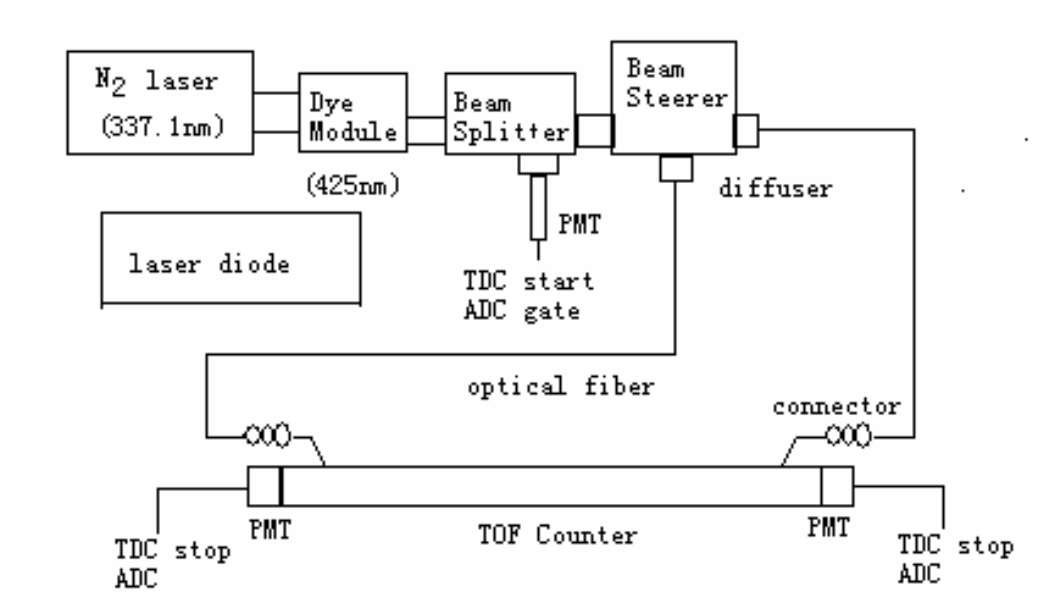

Figure 17: BESII TOF calibration system schematic. The PMT at the Beam Splitter is the reference PMT.

7.1 Laser

In BESII, a self-contained nitrogen dye laser, VSL-337ND, was used. It no longer works, so a new laser is required. However, we may be able to use other parts of the old system, such as the PMT(R2248), beam splitter, or beam steering mirror.

Specifications for both a nitrogen dye laser and a laser diode are given below. A nitrogen dye laser was used in the past, so we know it will work. However, a laser diode will be simpler to use and more reliable. Collaborators at the University of Tokyo are successfully using a laser diode to test BESIII TOF phototubes [17], demonstrating that a laser diode may also work in our application.

7.1.1 Nitrogen dye laser

One of the current products from Spectra Physics (VSL-337ND-S) is similar to the old one. A N2 dye laser has the advantages of high power, low price, and a controllable wavelength, but disadvantages of low frequency, poor pulse-to-pulse stability, and a short life (about 10^8 pulses or 2 years). In addition, there is continuous power fall off over the lifetime of the dye laser cartridge, requiring that the carcinogenic dye be constantly changed or that the amount of filtering be changed to compensate. Also the alignment of the N2 laser and dye laser is very sensitive, and frequent realignment is required.

The specifications for the N2 dye laser are given in Table 6. The price of the N2 dye laser is about $ 12,000.

7.1.2 Laser diodes

Two laser diode systems are being investigated. One is from Germany (PDL 800-B, PicoQuant GmbH), and the other is from Japan (PLP-10, Hamamatsu). Since they are rather similar, only the German laser will be described here. The laser head (LDH-P, PicoQuant GmbH) is shown in Fig. 18, and specifications for models with wavelengths in the region of interest are given in Tables 7 and 8. Specifications for the driver are given in Table 9. The system features short laser pulses, down to 50 ps (FWHM), repetition rates from single shot to 40 MHz, adjustable laser power and pulse width, and a

Table 6: Nitrogen dye laser specifications (VSL-337ND-S N2 laser with DUO220 dye laser).

Nitrogen laser	VSL-337ND-S
Pulse energy	300 μJ
Pulse to Pulse stability	4% std. dev.
Pulse width	< 4 ns
Repetition rate/burst	1-30 Hz/60Hz
Beam size	35 mm^2
Beam divergence, full angle	0.5 mrad, typ.
Average power @ 20Hz	6 mW
Dye laser	visible tunable DUO220
Spectral range	360 - 700 nm
Repetition rate	1 to 30 Hz
Pulse width (FWHM)	4 ns
Pulse energy	$> 70\mu$J at 500 nm
Pulse to pulse energy stability	6 % std. dev.
Peak power	> 18 kW at 500 nm
Average power at 20 Hz	> 1.4mW at 500 nm
Beam size	2 x 3 mm
Beam divergence	4 mrad

choice of laser heads with wavelengths from 280 to 600 nm. The LDH-P-C-405B laser diode has a peak power of 350 mW and is estimated to provide $\sim 5 \times 10^7$ photons per pulse at 405 nm wavelength (LDH-P-C-405B). The cost with driver is approximately $ 24,000.

The laser beam cross section is approximately 1.5 mm x 3.5 mm. PicoQuant GmbH offers a fiber coupling option and single mode cable that provide a circular beam for $ 3200 and $ 350, respectively. This system yields about 30 % of the original intensity. An additional option is an anamorphotic beam shaper ($ 700), used with the fiber coupling option, which yields 40 to 50 % of the original beam intensity. We budget for these options but will look into other possibilities. The total is $28,000.

Figure 18: German laser head (LDH-P, PicoQuant GmbH).

The schematic of the BESIII TOF calibration system with a laser diode is shown in Fig. 19. It is very similar to the system used in BESII, but we replace the nitrogen laser with a laser diode. Table 10 lists some estimated calibration system costs.

Table 7: German laser head specifications (LDH-P, PicoQuant GmbH). Only choices in the desired wavelength range are given.

Type	wavelength	Low power (Narrow Pulse)		High Power (wide Pulse)	
	($\pm$ 10 nm)	pulse (FWHM) (ps)	Average power 40MHz (mW)	pulse (FWHM) (ps)	Average power 40MHz (mW)
LDH-P-C-405	405	< 70	0.8	< 300	1.0
LDH-P-C-405B	405	< 70	1.0	< 300	3.0
LDH-P-C-440	440	< 90	0.3	< 300	1.0

Table 8: Laser head (LDH-P, PicoQuant GmbH) specifications: beam parameters.

Optics focus length	f' = 4.5 mm
Numerical aperture	0.55
Typical divergence	Theta parallel 0.32 mrad
(with optics)	Theta perpendicular 0.11 mrad
Cooling (optional)	
Peltier cooling stability	better than 1 K
Spectral Width	2-8 nm
Power Stability (cooled)	
12 hours, T ambient < 3 K	1% RMS
	3% Peak to Peak

Table 9: German diode laser driver specifications (PDL 800-B, PicoQuant GmbH).

Internal Clock:	
Master frequency	40 MHz crystal locked
Repetition frequencies	40, 20, 10, 5 or 2.5 MHz
External Trigger Input:	
Amplitude	-5 to +5 V(maximum limits)
Trigger level (adjustable)	-1 to +1V (negative slope)
Pulse width	$>$ 3 ns
Frequency range	10 Hz to 80 MHz
Impedance	50 Ohms
Synchronization Output:	
Amplitude	$<$ -800 mV into 50 Ohms (NIM)
Pulse width	5 ns
Impedance	50 Ohms

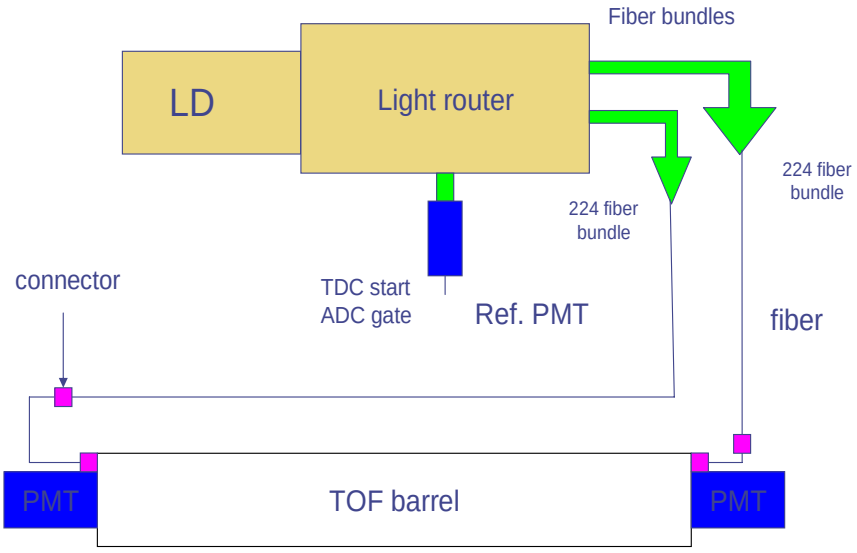

Figure 19: BESIII TOF calibration system schematic.

Table 10: Some estimated calibration system costs.

Component	Cost
Beam splitter	$ 1000
Beam steering mirror	1400
Neutral density filters (3)	360
PMT (2)	920
Diffuser (2)	150
Beam expander	700
Mechanical (brackets, bundle connector, etc.)	4000
Misc.	1000
Total	$ 9530

7.1.3 Laser beam measurements

It is important to be able to measure the size, beam shape, and intensity profile of the laser beam, before and after the optical system used to couple the beam into the fiber bundle. This may be done using a CCD camera connected to a PC via a Firewire connection. Such a system is available from Spiricon (www.spirocon.com). The LBA-FW-SCOR20, which includes camera and software is $4,995. Other items that may be necessary to expand the laser beam to match the CCD camera are a Beam Reducer and Expander BR-3X ($650), 50 mm CCTV Lens FL-50 ($195), and s 2" Opal Target with holder ($105).

7.2 Optical fibers

The optical fiber bundles used in BESII were destroyed. The bundles were constructed at UH. Each contained 46 telecommunication fibers, which were purchased from Fibertron, Inc. For BESIII, two fiber bundles will be ordered; each will have 224 fibers total; 176 for one end of the barrel TOF counters and 48 for one set of endcap TOF counters. The cores of all 224 fibers will be illuminated by the pulsed laser system. The fiber bundle cable will divide into barrel and endcap bundles. The individual fibers will connect to short fiber optic cables that plug into the TOF counters through a hole in the

phototube base as shown in Fig. 20. The fiber run is 18 m. The estimated cost of the fiber bundles, connectors, and short fiber optics cables is $80,000.

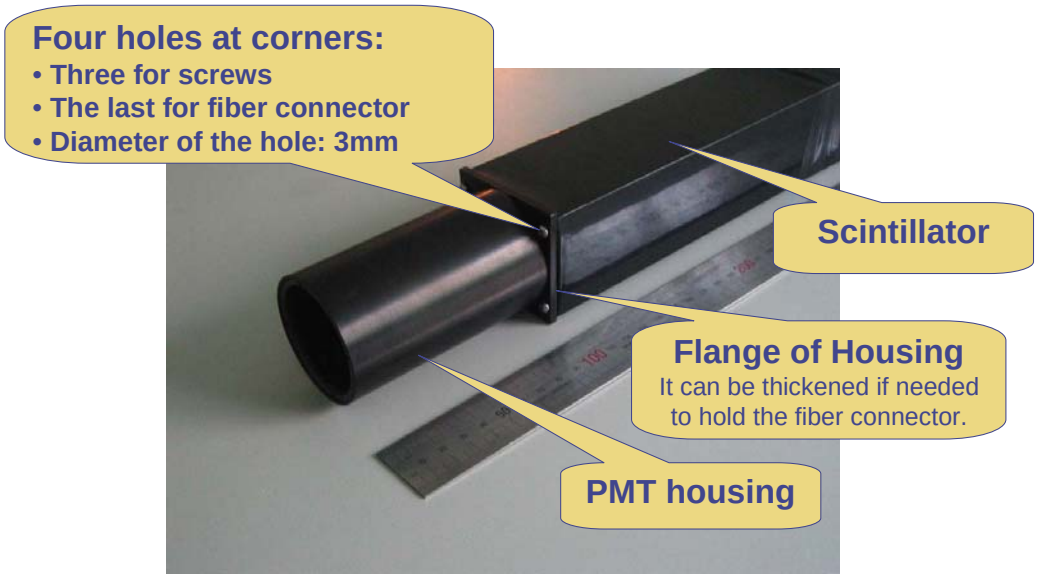

Figure 20: Fiber connection to TOF counter.

7.3 Tests of calibration system and TOF counters

We will test the TOF calibration system with a BESIII TOF counter. Since Belle is setting up a test stand to test the upgrade to Belle TOF counter electronics, we will make use of their setup but will have to buy more channels of TDC and ADC readout to carry out our tests. We will not only test the TOF calibration system, including the pulse shape, rise time, intensity distribution, optical fiber performance, etc., but also the TOF counter resolution and the BESIII electronics. We budget $ 5000 for additional electronics and HV channels, $ 2000 to construct a cosmic ray telescope for testing the BESIII TOF counter, and $ 1500 for a PC for data acquisition.

We will borrow a TOF counter and phototubes from IHEP, so we do not budget for these items but do include the cost of shipping.

8 The BES TOF Collaboration

The TOF system is being constructed at IHEP, and the TOF electronics are being developed at USTC. There will be close coordination between these TOF groups and the work on the TOF calibration system by the University of Hawaii. This can be accomplished with trips, email, and video conferencing, which has been used successfully in BESII.

The University of Hawaii group in this proposal includes professors F. Harris, S. Olsen, and G. Varner, postdoc Z. Guo, a graduate student Duc Ong, and engineer Marc Rosen. Marc played a major role in the construction of both the BESII and the Belle TOF calibration systems so his knowledge and participation here are very important to the success of this project.

Also very crucial to this proposal is that we plan to hire a postdoc for three years to play a key role in the construction and testing of the calibration system and to contribute much needed manpower to the effort. The postdoc will also participate in software development for the BESIII TOF system, as well as participate in BESII analysis.

BES will continue to be Harris' main research activity and, although Olsen's primary focus is the BELLE experiment, he will continue to contribute to the BES experiment. Olsen is planning a sabbatical in China in 2007, which should be extremely helpful to the start up of BESIII.

If the TOF calibration system proposal is approved, the Hawaii group will

assemble and test the system on a BESIII TOF counter at the University of Hawaii. The calibration system will then be sent to IHEP for installation, where it will become an important tool for monitoring the operation of the TOF system during and after installation, and helping to calibrate the TOF system during data taking.

9 Schedule

Time available for the construction of the TOF calibration system is extremely short. Assembly will begin as soon as the grant is awarded. An outline of our proposed schedule is shown in Table 11. It will take three months to procure most parts. During this time, we will set up the assembly area and construct and test the prototype TOF counter.

We plan on shipping the TOF monitoring system to IHEP by summer 2006.

Table 11: Proposed schedule for the TOF Calibration system.

2005	1 September	Research N2 vs. Diode Laser
		Design remainder of system
	15 October	Place orders for parts
	1 December	Complete TOF prototype module and test
		Begin Assembly of Calibration system
	1 January	Finish assembly, begin tests
2006	1 May	Testing complete
	1 June	Ship to IHEP

10 Budget Discussion

The costs of the TOF calibration system components and test setup have been estimated. These include the components, fabrication, fiber cables, and shipping of the completed parts to IHEP. The total estimated cost for these components is $124,530. The total cost including travel and a postdoc for

three years is $320,052. Postdoctoral fellowships at the University of Hawaii are considered traineeships and as such are not subject to overhead. We anticipate travel to China 4 times a year for the postdoctoral fellow. These estimates are summarized in Tables 12 to 15 (attached to the end of this proposal).

11 Summary

We propose to build a TOF calibration system for the BESIII experiment. The University of Hawaii has experience building such systems for BESII and Belle. However the laser from the BESII system no longer works, and it is not known if other parts of the system can be used. The TOF detector is being built at IHEP, while the TOF electronics is being developed at USTC. The TOF calibration system is essential to monitor the performance to the TOF system and to aid in its calibration. The TOF system is essential in BESIII for particle identification. The total amount requested for the US portion of this project is $320,052.

References

[1] J. Z. Bai, et al. (BES), *Measurement of the mass of the τ lepton*, Phys. Rev. **D53**, 20 (1996).

[2] J. Z. Bai, et al. (BES), *Determination of the J/ψ leptonic branching fractions via $\psi(2S) \to \pi^+\pi^- J/\psi$*, Phys. Rev. **D58**, 092006 (1998).

[3] J. Z. Bai, et al. (BES), *Measurement of the total cross section for hadronic production by e^+e^- annihilation at energies between 2.6 and 5 GeV*, Phys. Rev. Lett. **84**, 594 (2000).

[4] J. Z. Bai, et al. (BES), *Measurements of the cross section for $e^+e^- \to$ hadrons at center-of-mass energies from 2 to 5 GeV*, Phys. Rev. Lett. **88**, 101802 (2002).

[5] R. A. Briere, et al. (CLEO), *CLEO-C and CESR-C: A new frontier of weak and strong interactions*, CLNS-01-1742, (2001).

[6] N. Cabibbo, Phy. Rev. Lett. **10**, 531 (1963).

[7] M.Kobayashi and T.Maskawa, Prog. Theo. Phys. **49**, 652 (1973).

[8] P.Ruiz-Femenia and A.Pich, Phys. Rev. **D64**, 053001 (2001).

[9] C. Patrignani, "h_c searches at FNAL E835", Talk at Quarkonium Working Group Meeting, Beijing, China, Oct. 12 - 16, 2004.

[10] J. L. Rosner, et al. (CLEO), *Observation of h_c state of charmonium*, hep-ex/0505073 (2005).

[11] N.A.Toernqvist, Found. of Phys. **11**, 171(1981).

[12] G.Burdman et. al., Phys. Rev. **D66**, 014009 (2000).

[13] Chi Peng Cheng, and Hong Wei Zheng, Nucl. Instr. Meth. **A252**, 67-74 (1986).

[14] H. Kichimi et al, Belle Collab., "The Belle TOF system", Nucl. Instr. Meth. **A453**, 315 (2000).

[15] J. W. Nam et al., Belle Collab., "A detailed Monte Carlo simulation of the Belle TOF system", Nucl. Instr. Meth. **A491**, 54 (2002).

[16] J.Z. Bai et al., BES Collab., Nucl. Instr. Meth. **A458**, 627 (2001).

[17] T. Yamamura, "PMT performance test for BESIII TOF system", talk presented at BES Annual Meeting, China, May 30 - June 2, 2005.